Plant Molecular Biology **52:** 817–830, 2003.

Identification and molecular characterization of mitochondrial ferredoxins and ferredoxin reductase from *Arabidopsis*

Keiko Takubo[1], Tomomi Morikawa[1], Yasuki Nonaka[2], Masaharu Mizutani[3], Shigeo Takenaka[1], Keiji Takabe[4], Masa-aki Takahashi[1] and Daisaku Ohta[1,*]

[1]*Graduate School of Agriculture and Biosciences, Osaka Prefecture University, 1-1 Gakuen-cho, Sakai 599-8531, Japan (*author for correspondence; e-mail ohtad@plant.osakafu-u.ac.jp);* [2]*Graduate School of Nutrition, Koshien University, Momijigaoka, Takarazuka 665-0006, Japan;* [3]*Institute for Chemical Research, Kyoto University, Gokasho Uji, Kyoto 611-0011, Japan;* [4]*Graduate School of Agriculture, Kyoto University, Kyoto 606-8502, Japan*

Received 17 November 2002; accepted in revised form 12 April 2003

Key words: Arabidopsis, ferredoxin, ferredoxin reductase, mitochondria

Abstract

We have identified and characterized novel types of ferredoxin and ferredoxin reductase from *Arabidopsis*. Among a number of potential ferredoxin reductase genes in the *Arabidopsis* genome, *AtMFDR* was identified to encode a homologue of mitochondrial ferredoxin reductase, and *AtMFDX1* and *AtMFDX2* were predicted to code for proteins similar to mitochondrial ferredoxin. First, we isolated cDNAs for these proteins and expressed them in heterologous systems of insect cells and *Escherichia coli*, respectively. The recombinant AtMFDX1 and AtMFDR proteins exhibited spectral properties characteristic of ferredoxin and ferredoxin reductase, respectively, and a pair of recombinant AtMFDX1 and AtMFDR proteins was sufficient to transfer electrons from NAD(P)H to cytochrome *c in vitro*. Subcellular fractionation analyses suggested membrane association of AtMFDR protein, and protein-gel blot analyses and transient expression studies of green fluorescence protein fusions indicated mitochondrial localization of AtMFDX1 and AtMFDR. RNA-gel blot analyses revealed that the accumulation levels of *AtMFDXs* and *AtMFDR* gene transcripts were specifically high in flowers, while protein-gel blot analysis demonstrated substantial accumulation of AtMFDR protein in leaf, stem, and flower. Possible physiological roles of these mitochondrial electron transfer components are discussed in relation to redox dependent metabolic pathways in plants.

Introduction

Mitochondrial ferredoxin and ferredoxin reductase are involved in a variety of redox reactions in the cell (Arakaki *et al*., 1997). Adrenodoxin (ADX) is a [2Fe-2S]-type mitochondrial ferredoxin, mediating electron transfer from NADPH via adrenodoxin reductase (ADR) to the terminal electron acceptor, cytochrome P450 (P450) monooxygenases in mitochondria (Grinberg *et al*., 2000). In vertebrates, these mitochondrial P450s catalyze the reactions of the cholesterol side chain cleavage and the steroid hydroxylation in the steroidogenic tissues (Vickery, 1997). Yeast mitochondrial proteins, Yah1p (Barros and Nobrega, 1999) and Arh1p (Lacour *et al*., 1998; Manzella *et al*., 1998), correspond to ADX and ADR homologues, respectively. However, in yeast, no mitochondrial P450s are present, but Yah1p (Lange *et al*., 2000) and Arh1p (Li *et al*., 2001) have recently been characterized to participate in the processes of Fe-S cluster maturation and mitochondrial iron homeostasis. Prokaryotic microorganisms also synthesize Fe-S clusters (Takahashi and Nakamura, 1999; Lill and Kispal, 2000) through the functions of a series of proteins including [2Fe-2S] ferredoxin. Furthermore, it has recently been reported that mitochondrial ferredoxin was involved in heme A synthesis in yeast (Barros *et al*., 2002).

In plants, multiple redox proteins have been studied as electron transfer components in microsomal P450 monooxygenase systems (Urban *et al*., 1997; Mizutani and Ohta, 1998; Fukuchi-Mizutani *et al*.,

1999). On the other hand, neither mitochondrial P450 nor electron transfer systems containing mitochondrial ferredoxin and its reductase has been characterized in plants. However, based on BLAST searches with bovine ADX and ADR protein sequences at the Arabidopsis Information Resource (http://www.arabidopsis.org/), we were able to identify two predicted genes potentially encoding proteins AtMFDX1 and AtMFDX2 highly similar to ADX and a putative gene coding for a protein AtMFDR exhibiting homology to ADR. In this study, we clarified whether or not these putative genes were actually transcribed and examined if the gene products were functionally active in transferring electrons from NAD(P)H to P450s *in vitro*. Thus, by isolating cDNAs and producing recombinant proteins, we demonstrated that a pair of AtMFDX1 and AtMFDR proteins was capable of reducing cytochrome *c* (Cyt *c*) in the presence of NAD(P)H as the electron donor, and protein-gel blot analyses and transient expression of signal peptide-green fluorescence protein (GFP) fusions indicated mitochondrial localization of these electron transfer components. We discuss the possibilities of mitochondrial P450-dependent monooxygenase systems and other unidentified redox pathways containing AtMFDXs and AtMFDR in plants.

Materials and methods

Plant materials

Arabidopsis thaliana ecotype Columbia (Col-0) seedlings (Lehle Seeds, Round Rock, TX) were grown under conditions described previously (Mizutani and Ohta, 1998).

Isolation of AtMFDX1 *and* AtMFDX2 *cDNAs*

A BLASTP search was done at the Arabidopsis Information Resource with a bovine adrenocortical ferredoxin precursor protein sequence (GenBank accession number AAA30358), and two putative genes were found to encode ADX homologues in *Arabidopsis* (AT4g05450 and AT4g21090). An expressed sequence tag (EST) entry (GenBank accession number AV559714) was identified to contain a part of the coding sequence (CDS) of AT4g05450. cDNA clones encoded by the putative CDS of AT4g05450 were isolated by PCR with combinations of forward primers (X1F1, 5′-CAGTGAACGATGATCGGTCATA-3′; X1F2, 5′-ATGATCGGTCATAGGATCTCAAG-3′) and reverse primers (X1R1, 5′-ACTAATGAGGTTTTGGAACA-AAC-3′; X1R2, 5′-CTCCAATAGAAACATAATCA-TC-3′). pBluescript II (Stratagene, La Jolla, CA) phagemids were prepared from a λZapII cDNA library constructed from 7-day old *Arabidopsis* seedlings (Mizutani and Ohta, 1998) and were used as the template for PCR. The 5′ region of AT4g05450 transcripts was determined with a Marathon cDNA Amplification Kit (Clontech, Palo Alto, CA). On the other hand, several EST sequences (GenBank accession numbers AV552737, AV544248, and AI998580) were thought to have been derived from the gene annotation of AT4g21090. Sequence comparison with other mitochondrial ferredoxins indicated that the annotation of AT4g21090 is lacking its actual N-terminal portion, and the open reading frame (ORF) was corrected to encode a polypeptide of 198 amino acids. A cDNA clone containing the full-length ORF determined from AT4g21090 and AV552327 was synthesized by reverse transcription (RT)-PCR. Total RNA from flowers was used for the RT reaction with Superscript II (Invitrogen, Carlsbad, CA) and oligo$(dT)_{16}$ as the reverse primer. PCR was done with a set of PCR primers, X2F1 (5′-CGATTCTAGAATGGTCTTCCATAGGCTATC-3′) and X2R1 (5′-CGTTTCTAGAGTGAGGTTTTGG-AACAAAC-3′). PCR products were cloned into the pGEM-T Easy vector system II (Promega, Madison, WI) to obtain pAtMFDX1 for AT4g05450 and pAtMFDX2 for AT4g21090. The GenBank/EMBL/DDBJ accession numbers for AtMFDX1 and AtMFDX2 cDNAs encoding the *Arabidopsis* ADX homologues were AB07538 and AB081937, respectively.

Isolation of AtMFDR *cDNA*

A protein sequence of bovine NADPH:adrenodoxin oxidoreductase (Nonaka *et al*., 1987) was used for a BLASTP search, and the CDS for a putative NADPH-ferredoxin oxidoreductase (AT4g32360) was identified. A full-length cDNA encoded by AT4g32360 was obtained by RT-PCR with total RNA from 4-week old plants and a set of PCR primers, ANR-F1 (5′-ATGAGTAGATATCTAGCAAG-3′) and ANR-R2 (5′-CTAGTTGGCTGCTGCTGCTAA-3′). The PCR product was cloned into a pGEMT-easy vector (Promega) to obtain pAtMFDR. Sequence analysis of pAtMFDR revealed that the gene annotation of AT4g32360 was missing an additional exon between the predicted exons 4 and 5, and an ORF of

AtMFDR transcript was thus determined to be 1452 bp long. The GenBank/EMBL/DDBJ accession number of AtMFDR cDNA is AB07540.

Heterologous expression of AtMFDR *cDNA in insect cells*

Recombinant AtMFDR protein was produced by expressing the entire coding region of AtMFDR cDNA with a baculovirus expression vector system as described previously (Mizutani *et al*., 1997). Briefly, AtMFDR cDNA was amplified by PCR with a primer set of FNRBF (5′-TACGGGATCCATGGTGTCTAGATACTTCTCTTC-3′) and FNRBR (5′-CAGCCAAGCTTGTCAATGATGATGATGATGATGATGTCCGTTGGCTGCTGCTG-3′). FNRBF contained a *Bam*HI restriction site (underlined), and FNRBR contained a *Hin*dIII restriction site (underlined) with the oligonucleotide sequence (double-underlined) to add a 6× His tag to the C-terminus of the protein. The PCR product was double-digested with *Bam*HI and *Hin*dIII and inserted into the *Bam*HI-*Hin*dIII site of pFASTBAC plasmid (Invitrogen). Preparation of the recombinant baculovirus DNA containing AtMFDR cDNA and transfection of insect cells (Sf9, Invitrogen) were done according to the manufacturer's instructions. The infected Sf9 cells were sonicated and centrifuged at 100 000 × *g* for 1 h. The pellet was homogenized with buffer A containing 20 mM potassium phosphate pH 7.25, 20% glycerol, 1 mM dithiothreitol, and 10 μM FAD, and proteins were solubilized in buffer B containing the same constituents as buffer A supplemented with 1% w/v Emulgen 913 (Kao Atlas, Tokyo, Japan). After centrifugation at 100 000 × *g* for 1 h, the solubilized recombinant AtMFDR (rAtMFDR) was purified with the aid of the C-terminal 6× His tag with NiNTA Agarose according to the manufacturer's instructions (Qiagen, Tokyo, Japan). The purified rAtMFDR protein was used to prepare rabbit anti-rAtMFDR antibodies.

Expression and purification of recombinant AtMFDX1 protein

Expression and purification of rAtMFDX1 was done with the pGEX-6P-1 vector system (Amersham Biosciences, Buckinghamshire, UK). A cDNA fragment encoding a mature form of AtMFDX1 (without the N-terminal 70 amino acids) was amplified by PCR with the full-length AtMFDX1 cDNA as the template and a primer set of MFDXf2 (5′-CCCTGGGATCCTCCTCTGAGAATGGTGATG-3′) containing a *Bam*HI site (underlined) and MFDXr (5′-TATTGACCCGGGCTAATGAGGTTTTGGAAC-3′) containing a *Sma*I site (underlined). The amplified PCR product was double-digested with *Bam*HI and *Sma*I and cloned into a pGEX-6P-1 vector to obtain an expression plasmid. An *Escherichia coli* strain, BL21 (DE3), was transformed with the expression plasmid for the production of recombinant AtMFDX1 (rAtMFDX1) as a fusion with a glutathione *S*-transferase (GST) protein according to the manufacturer's instructions. The transformed *E. coli* cells were homogenized with PBS (potassium-buffered saline, Takara Shuzo, Kyoto, Japan) containing a protease inhibitor cocktail comprising 4-(2-aminoethyl)benzenesulfonyl fluoride, pepstatin A, bestatin, and Na-EDTA (Sigma Aldrich Japan, Tokyo). The AtMFDX1-GST fusion protein was obtained with Glutathione Sepharose 4B (Amersham Biosciences), and a mature form of AtMFDX protein was purified after the cleavage with PreScission Protease (Amersham Biosciences) according to the manufacturer's protocols.

Subcellular fractionation and protein blot analysis

Chloroplasts and mitochondria were prepared basically according to the methods described by Kunst (1998) and Klein *et al*. (1998), respectively. All procedures were done at 4 °C. Briefly, 10 g of leaf tissue was homogenized with an extraction buffer containing 0.45 M sorbitol, 20 mM Tricine-KOH pH 8.4, 5 mM EDTA, 5 mM EGTA, 10 mM Na_2CO_3, 10 mM dithiothreitol (DTT), 1 mM phenylmethylsulfonyl fluoride (PMSF), a protease inhibitor cocktail containing 4-(2-aminoethyl)benzenesulfonyl fluoride, pepstatin A, bestatin, and Na-EDTA (Sigma Aldrich), 0.2% w/v bovine serum albumin, and 0.6% w/v polyvinylpyrrolidone with a homogenizer (IKA Works, S25 KR-25F, Wilmington, NC). Crude chloroplasts were precipitated from 100 × *g* supernatant by centrifugation at 2000 × *g* for 2 min. The chloroplast pellet was re-suspended in a buffer containing 40% w/v Percoll (Amersham Biosciences), 0.45 M sorbitol, 20 mM Tricine-KOH pH 7.6, 5 mM EDTA, 5 mM EGTA, 10 mM Na_2CO_3, 10 mM DTT, and 1 mM PMSF. The chloroplast suspension was then loaded onto a 40%/50%/70% v/v Percoll step gradient in a buffer consisting of 0.45 M sorbitol, 20 mM Tricine-KOH pH 7.6, 5 mM EDTA, 5 mM EGTA, 10 mM Na_2CO_3, 10 mM DTT, and 1 mM PMSF. After

centrifugation at 6000 × *g* for 15 min, intact chloroplasts were collected at the 50%/70% interface and washed by centrifugation at 2000 × *g* for 10 min in a buffer containing 0.3 M sorbitol, 50 mM Tricine-KOH pH 7.6, 10 mM NaCl, 2 mM EDTA, 1 mM $MgCl_2$, and 0.5 mM KH_2PO_4. Mitochondria were purified from the 2000 × *g* supernatant obtained during the chloroplast isolation process. The supernatant was centrifuged at 6000 × *g* for 5 min, and the obtained supernatant was further centrifuged at 16 000 × *g* for 15 min to pellet the crude mitochondrial fraction. Then, the mitochondrial pellet was re-suspended in a buffer consisting of 0.45 M sorbitol, 20 mM Tricine-KOH pH 7.6, 5 mM EDTA, 5 mM EGTA, 10 mM DTT, and 1 mM PMSF. The mitochondrial suspension was layered onto a Percoll step gradient of 18%/23%/40% v/v and centrifuged at 12 000 × *g* for 30 min. The mitochondria collected at the 23%/40% interface were suspended in a buffer containing 0.35 M sorbitol, 50 mM Tricine-KOH pH 7.6, 2 mM EDTA, 2 mM EGTA, and 1 mM PMSF. The intactness of chloroplasts and mitochondria was judged from the oxygen evolution activity with ferricyanide as the Hill oxidant (Walker, 1980) and the latency of Cyt *c* oxidase (Neuberger *et al*., 1982; Krömer and Heldt, 1991), respectively. Protein samples (20 μg) were separated by SDS-PAGE (Laemmli, 1970) and electroblotted onto a polyvinylidene difluoride membrane (Immobilon P; Millipore, Bedford, MA). The membrane was incubated with the anti-rAtMFDR antibodies (1:3000 dilution), and immunoreactive proteins were detected using the ECL western analysis system (Amersham Biosciences). Rabbit anti-spinach ribulose-bisphosphate carboxylase (Rubisco) antibodies (a gift from A. Yokota, Nara Institute for Science and Technology, Japan) at 1:6000, and rabbit anti-citrate synthase antibodies (Koyama *et al*., 1999) at 1:2000 were also used for immunoblotting. For tissue immunolabeling experiments, *Arabidopsis* leaf sections were embedded in LR-White resin (Oken-Shoji, Tokyo, Japan) after the fixation in 50 mM potassium phosphate buffer pH 7.4 containing 16% w/v paraformaldehyde and 2% w/v glutaraldehyde. The anti-AtMFDR antiserum and the rabbit anti-spinach Rubisco antibodies were used as the primary antibodies, and Cy3-labeled goat anti-rabbit IgG (Jackson Immunoresearch Laboratories, Westgrove, PA) was used for the detection of the primary antibodies. Immunofluorescent images were collected using a fluorescence microscope (Eclipse E600, Nikon, Tokyo, Japan).

Transient expression and localization studies in onion epidermal cells

Putative signal peptide sequences were PCR-amplified from full-length cDNA clones of AtMFDXs and AtMFDR with pairs of primers as follows: Met-1 to Ile-93 of AtMFDX1, 5′-CAGTCGACATGATCGGTCATAGGATCTCAAG-3′ and 5′-GACCATGGGAATTTCCTCTCCGTCCTTATCAAC-3′; Met-1 to Ile-93 of AtMFDX2, 5′-CAGTCGACATGGTCTTCCATAGGCTATCAAGA-3′ and 5′-GACCATGGGAATTTCCTCTCCATCTTTATCAA-3′; Met-1 to Val-40 of AtMFDR, 5′- CAGTCGACATGAGTAGATATCTAGCAAG-3′ and 5′-GACCATGGGTACCTTGTCAGCAGTATAGAAAC-3′. The upstream primers and the reverse primers contained *Sal*I sites (underlined) and *Nco*I sites (double-underlined). The amplified fragments were cloned in-frame upstream of the green fluorescent protein sGFP(S65T) reading frame (Chiu *et al*., 1996) with a *Sal*I-*Nco*I restriction site to obtain AtMFDX/S-GFP and AtMFDR/S-GFP. For transient expression in onion epidermal cells, 25 μl of gold particles (1 μm diameter in 20% glycerol) were mixed with 5 μg of plasmid DNA, 50 μl of 2.5 M $CaCl_2$, and 25 μl of 0.1 M spermidine. Aliquots of gold were spotted on macrocarriers and used to transform tissues at 7.6 MPa with a PDS 1000HE biolistic device (BioRad, CA). MitoTracker Red staining was done according to the protocol given by the manufacturer (Molecular Probes, Eugene, OR). Fluorescence of sGFP(S65T) and Mitotracker Red CMXRos was visualized under an Olympus microscope IX71 (Olympus, Tokyo, Japan) equipped with filter sets of U-MGFPHQ for sGFP and U-MWIG2 for MitoTracker. Images were taken with the DP manager software (Olympus).

Preparation and analyses of RNA

Preparation and analysis of RNA were done as described previously (Fujimori and Ohta, 1998). Total RNA (10 μg) was analyzed by northern hybridization using full-length cDNAs of AtMFDX1 and AtMFDR labeled with [α-^{32}P]dCTP. Blots were analyzed with a Bio Imaging Analyzer, FLA3000 (Fuji Photo Film, Tokyo). RT-PCR analyses were designed for a detailed comparison of tissue-specific expression of *AtMFDX1* and *AtMFDX2* genes. Thus, first-strand cDNAs were synthesized with total RNA (5.0 μg) from various tissues, Superscript II (Invitrogen), and oligo(dT)$_{16}$ as a reverse primer. PCR

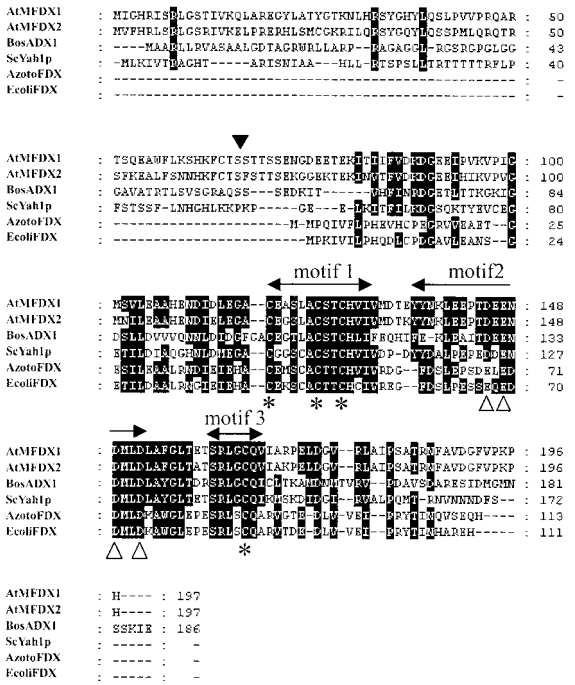

Figure 1. Alignment of amino acid sequences of ferredoxin proteins. The deduced amino acid sequences of AtMFDX1 and AtMFDX2 proteins are aligned with other ferredoxin proteins; BosADX1 (*Bos taurus* ADX1, AAA30357), ScYah1p (*Saccharomyces cerevisiae* Yah1p, NP_015071), AzotoFDX (*Azotobacter vinelandii* Fdx, AAC24477), and EcoliFDX (*Escherichia coli* FDX, NP_289082). The arrows above the sequences indicate the conserved motifs containing the acidic amino acid residues (pointed by a white upward arrowhead) proposed to be involved in the interaction with the reductase and the conserved Cys residues for the [Fe-S] cluster binding (indicated by asterisks) (Ziegler *et al*., 1999; Grinberg *et al*., 2000; Ziegler and Schultz, 2000). The back downward arrowhead indicates the position corresponding to the N-terminus of the mature form of mammalian ADX proteins. Dashes indicate gaps inserted to allow optimal sequence alignment. Conserved amino acid residues were shaded. The sequences of AtMFDX1 and AtMFDX2 have been submitted to the GenBank/EMBL/DDBJ databases under accession numbers AB07538 and AB081937, respectively.

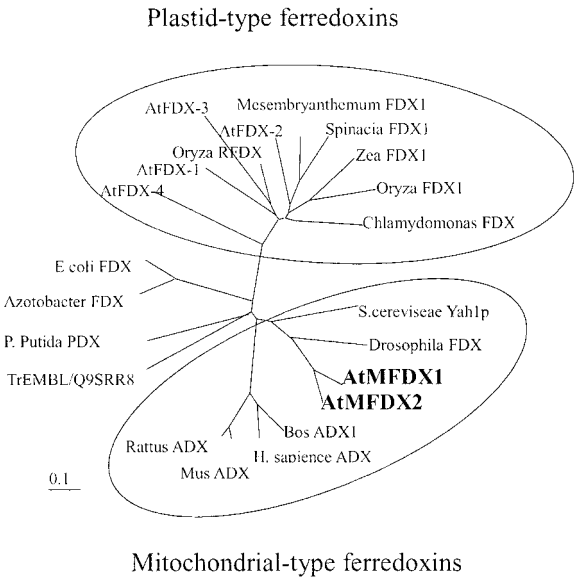

Figure 2. Phylogenetic tree for ferredoxin proteins. The clustalW program was used for the analysis of AtMFDX1 (AB07538), AtMFDX2 (AB081937), *Arabidopsis* ferredoxins (AtFDX-1, AAD15602; AtFDX-2, AAB65481; AtFDX-3, BAB09421; AtFDX-4, CAB10628; Q9SRR8, AAK62394), *A. vinelandii* Fdx (AAC24477), *B. taurus* ADX1 (AAA30358), *Chlamydomonas reinhardtii* FDX (AAC49171), *Drosophila melanogaster* Fdx (AAF50293), *Escherichia coli* FDX (NP_289082), *Homo sapiens* ADX(NP_004100), *Mesembryanthemum crystallinum* ferredoxin I precursor (AAB61593), *Mus musculus* ADX (NP_032022), *Oryza sativa* RFDX (BAA19865), *O. sativa* FDX1 (AAB65699), *Rattus norvegicus* ADX (P24483), *Spinacia oleracea* FDX1 (AAA34028), *Pseudomonas putida* PDX(BAA00414), *S. cerevisiae* Yah1p (NP_015071), and *Zea mays* FDX1(AAA33460). The GenBank/EMBL/DDBJ accession numbers for the proteins are indicated in parenthesis. AtMFDX1 (AB07538) and AtMFDX2 (AB081937) are shown in bold type.

was done with rTaq DNA Polymerase (Toyobo, Osaka, Japan) and a combination of gene-specific primer sets. The set for AtMFDX1 was Adx3′-FW (5′-CCAACAGATGAAGAGAATGATATGC-3′) and Adx1-3′-RV (5′-CGCTTGTTGTTCTGTTAGAAACTC-3′), and a set of Adx3′-FW (5′-CCAACAGATGAAGAGAATGATATGC-3′) and Adx2-3′-RV (5′-CTGATCAGAACCAAGTCAGGC-3′) was for AtMFDX2. The sequences of the forward primer (Adx3′-FW) and the reverse primers (Adx1-3′-RV and Adx2-3′-RV) were from exon 6 and the 3′ non-coding region of the AtMFDX genes, respectively. Accordingly, the amplification from genomic DNA should be distinguished from RT-PCR products, if any, by checking the presence of the additional intron sequence located between exon 6 and exon 7. The *Arabidopsis* actin gene (*AAc1*, Nairn *et al*., 1988) was amplified by RT-PCR as an internal control with a primer pair of Act-F (5′-ATGGCTGATGGTGAAGACATTC-3′) and Act-R (5′-TCAGAAGCACTTCCTGTGAAC-3′). PCR products were analyzed on a 1.0% agarose gel and their identity to the original sequence was confirmed by DNA sequencing.

DNA sequence analysis

DNA sequences were determined from both strands with CEQTM DTCA-Quick Start Kits (Beckman Coulter, Fullerton, CA) and a DNA sequencer, CEQTM2000XL DNA Analysis System (Beckman Coul-

ter). DNA and amino acid sequences were analyzed with GENETYX software (Software Development, Tokyo, Japan). Amino acid sequences were aligned by the ClustalW program (Thompson *et al*., 1994), and phylogenetic trees were constructed by with the PHYLIP program, ver. 3.5c (Felsenstein, 1996).

Assay methods

The rAtMFDX1 content was determined from the absorbance maximum (414 nm) with an extinction coefficient (ϵ = 9.8 mM^{-1} cm^{-1}; Huang and Kimura, 1973). The concentration of rAtMFDR was determined from the absorbance maximum (450 nm) of the oxidized form with an extinction coefficient (ϵ = 10.9 mM^{-1} cm^{-1}; Chu and Kimura, 1973). Reactions of Cyt *c* reduction/oxidation were done at 30 °C in an assay mixture (1 ml) containing 50 mM potassium phosphate buffer pH 7.4, 20 μM Cyt *c*, concentrations of either NADH or NADPH, rAtMFDX1 protein, and rAtMFDR protein. Reaction rates were determined by following absorbance changes at 550 nm (ϵ = 19.1 mM^{-1} cm^{-1}). The ferricyanide reduction rate was calculated with ϵ = 1.012 mM^{-1} cm^{-1} (Huang and Kimura, 1973) by monitoring the absorption decrease at 420 nm. The reaction was done at 30 °C in an assay mixture (1 ml) containing 50 mM potassium phosphate buffer pH 7.4, 200 μM potassium ferricyanide, varied concentrations of either NADH or NADPH, and rAtMFDR protein.

Results

Cloning of cDNAs for mitochondrial ferredoxin homologues from Arabidopsis

We isolated *AtMFDX1* and *AtMFDX2* cDNAs corresponding to the predicted coding sequences of AT4g05450 and AT4g21090, respectively (Figure 1). The AtMFDX1 cDNA contained an ORF of 594 bp encoding a polypeptide of 198 amino acids with a calculated molecular mass of 21 830 Da. A full-length AtMFDX2 cDNA was also isolated by RT-PCR using total RNA from flowers, and the ORF was predicted to encode a polypeptide with a molecular mass of 22 121 Da (Figure 1). The deduced primary structures of AtMFDX1 and AtMFDX2 proteins were 76% identical and exhibited strong sequence similarity to ADX proteins from other organisms. Namely, AtMFDX1 and AtMFDX2 protein sequences were 43% and 41% identical to that of bovine ADX1 (Kagimoto *et al*., 1988), respectively, and they were 52% and 43% identical to yeast Yah1p protein (Barros and Nobrega, 1999), respectively. The bovine ADX1 precursor sequence (Figure 1) contains the mitochondrial transport signal of 58 amino acids at its N-terminus (Grinberg *et al*., 2000), and the N-terminal extension of yeast Yah1p protein is involved in the mitochondrial matrix localizat ion (Barros and Nobrega, 1999). Between AtMFDX1 and AtMFDX2 proteins, no sequence similarity was evident in the N-terminal 60 amino acids, although they share 86% sequence identity when compared without the N-terminal regions. Mitochondrial localization of these ferredoxin isoforms from *Arabidopsis* was predicted with high probabilities by the PSORT program (http://psort.nibb.ac.jp/) and the TargetP (http://www.cbs.dtu.dk/services/TargetP/). It is possible that the N-terminal portions of AtMFDX1 and AtMFDX2 proteins may contain sequence information to determine their subcellular localization. On the other hand, the C-terminal regions of AtMFDX proteins were highly homologous to those of yeast Yah1p and mammalian ADX proteins (Figure 1) containing the four conserved Cys residues in motif 1 and motif 3 (Cys-118, Cys-124, Cys-127, and Cys-165) involved in the binding of the [2Fe-2S] cluster (Ziegler *et al*., 1999). The acidic amino acid residues (Asp-145, Glu-146, Asp-149, and Asp-152) implicated in the interaction with ferredoxin reductase protein (Grinberg *et al*., 2000; Ziegler and Schultz, 2000) were found in motif 2. Figure 2 shows a phylogenetic tree obtained with mitochondrial ferredoxin sequences, various plant-type ferredoxins, and ferredoxin sequences from microorganisms. Mitochondrial-type ferredoxins formed a cluster, which was clearly distant from that composed of plastidal ferredoxins. AtMFDXs and yeast Yah1p were in the group of mitochondrial-type ferredoxins.

A cDNA for a mitochondrial ferredoxin oxidoreductase homologue from Arabidopsis

BLASTP searches with a bovine ADR protein sequence (Nonaka *et al*., 1987) led to the identification of a putative gene, AT4g32360, potentially encoding a protein similar to ferredoxin-$NADP^+$ reductase. A full-length cDNA (AtMFDR) isolated by RT-PCR contained an ORF of 1452 bp for a polypeptide of 484 amino acids with a calculated molecular mass of 53 069 Da (Figure 3). The deduced primary structure of AtMFDR protein was 40.5% identical to that of bovine ADR, 40% identical to *Drosphila* ADR, and

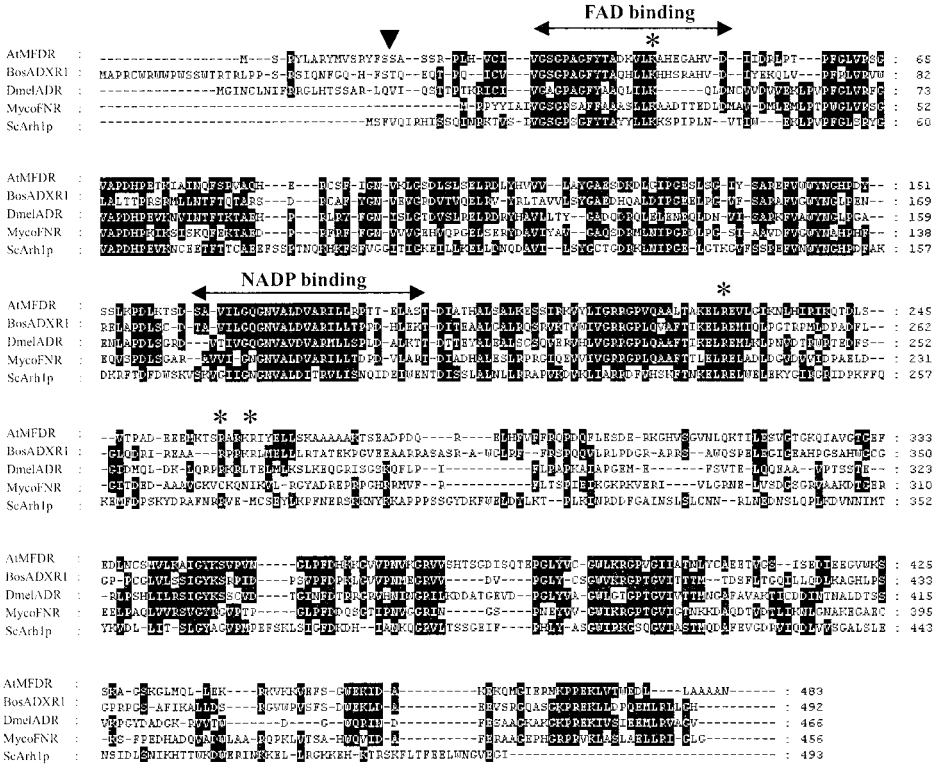

Figure 3. Alignment of amino acid sequences of ferredoxin reductase proteins. The predicted AtMFDR protein sequence is aligned with other ferredoxin reductase sequences. BosADXR1 (*B. taurus* ADXR1, AAA30362), DmelADR (*D. melanogaster* ADR, AAD50819), MycoFNR (*Mycobacterium tuberculosis* FNR, AAK47528), and ScArh1p (*S. cerevisiae* Arh1p, AAC49500) are included in the comparison. The arrows above the sequences indicate the FAD binding site and NADP binding site conserved among ferredoxin reductase (Arakaki *et al*., 1997), respectively. The positively charged amino acid residues involved in the interaction with ADX (Müller *et al*., 2001) are indicated by asterisks. Dashes indicate gaps inserted to allow optimal sequence alignment. Conserved amino acid residues were shaded. The black arrowhead indicates the N-terminus of the mature form of bovine ADR. The AtMFDR cDNA sequence has been deposited to the GenBank/EMBL/DDBJ databases under the accession number AB07540.

32% to yeast Arh1p, while it was about 19% identical to the plastidal NADPH-ferredoxin reductases from *A. thaliana*, *Spinacia oleracea*, *Oryza sativa*, and *Zea mays*. AtMFDR protein conserved two sequence motifs corresponding to the flavin binding domain and the NADP binding domain (Figure 3), respectively (Arakaki *et al*., 1997). The positively charged residues involved in the interaction with ADX and mitochondrial P450s (Müller *et al*., 2001) were also found as Lys-42, Arg-227, Arg-258, and Arg-262. In a phylogenetic tree (Figure 4), AtMFDR was grouped into a cluster of ferredoxin reductases involved in the electron transfer to mitochondrial P450s, while other plastidal ferredoxin reductases were in a separate group.

Characterization of recombinant AtMFDR protein

Full-length cDNA for AtMFDR was expressed in insect cells using a baculovirus expression vector system. SDS-PAGE analysis (Figure 5A) showed that a new intense band of about 55 kDa appeared in the insect cells infected with the recombinant virus containing the AtMFDR cDNA (Figure 5A, lanes 3 and 4). The apparent molecular mass of the expressed protein was in good agreement with the one calculated from the primary structure of AtMFDR protein (53 069 Da). The rAtMFDR protein recovered in the membrane fraction (Figure 5A, lane 4, the 100 000 × *g* pellet) was purified to apparent homogeneity using a metal chelating affinity column with the aid of the C-terminal His-tag (Figure 5A, lane 5). The rAtMFDR protein exhibited an absolute absorption spectra characteristic of flavoproteins (Figure 5B). The oxidized form showed prominent peaks at around 463 and 380 nm, typical of a flavoprotein. The 463 nm peak almost disappeared when reduced by adding the excess of NADPH and was completely abolished by the addition

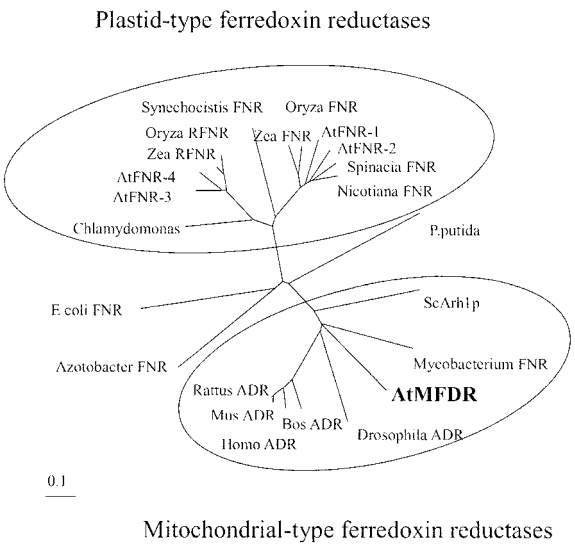

Figure 4. Phylogenetic tree for ferredoxin reductase proteins. The clustalW program was used for the analysis of AtMFDR protein sequence with the sequences of *A. thaliana* ferredoxin reductases (AtFNR1, AAF79911; AtFNR2, CAB52472; AtFNR3, CAB81081; AtFNR4, NP_174339), *A. vinelandii* FNR (AAA83029), *B. taurus* ADR1 (AAA30362), *C. reinhardtii* FNR (AAA79131), *D. melanogaster* ADR (AAD50819), *E. coli* FNR (CAA66094), *H. sapiens* ADR1 (AAB59497), *M. musculus* ADR (BAA08659), *M. tuberculosis* FNR (AAK47528), *N. tabacum* FNR (CAA74359), *O. sativa* FNR (BAA90642), *O. sativa* RFNR (BAA07479), *P. putida* PNR (BAA00413), *R. norvegicus* ADR (BAA23759), *S. oleracea* FNR (AAA34029), *Synechocystis* sp. PCC 6803 (NP_441779), *S. cerevisiae* Arh1p (AAC49500), *Z. mays* FNR (BAA88236), and *Z. mays* RFNR (AAB40034). The GenBank/EMBL/DDBJ accession numbers for the proteins are indicated in parenthesis. AtMFDR protein is indicated in bold type.

of sodium hydrosulfite (Figure 5B). The apparent K_m values for NADPH and NADH were determined to be 11.3 μM and 123 μM, respectively, using potassium ferricyanide as the electron acceptor. These K_m values were relatively higher than those of ADR proteins from other organisms, while the preference of NADPH over NADH was consistent with the reported properties (Grinberg *et al.*, 2000). These results indicated that the AtMFDR cDNA encoded a functionally active NAD(P)H-dependent oxidoreductase in *Arabidopsis*. The rAtMFDR protein was used as the antigen to prepare polyclonal antibodies for subcellular localization studies, and specificity of anti-rAtMFDR antibodies was examined using the crude extract from the insect cells expressing rAtMFDR. The anti-rAtMFDR antibodies were specific towards rAtMFDR, while some degradation products were also detected (Figure 5A, lane 7).

Electron transfer activity of AtMFDX and AtMFDR

A mature form of AtMFDX1 protein (rAtMFDX) was expressed as a fusion protein with a GST (Figure 6A). After protease treatment, rAtMFDX protein (ca. 20 kDa) was further purified with Glutathione Sepharose 4B (Figure 6A, lane 4). The UV-visible spectra of rAtMFDX1 exhibited the absorption maxima at 276, 322, 414, and 456 nm, which are characteristic of [2Fe-2S] type ADXs (Figure 6B). The spectral properties were closely similar to those reported for a human mitochondrial ferredoxin recombinantly produced in an *E. coli* system (Xia *et al.*, 1996), and a pair of rAtMFDX1 and rAtMFDR proteins was sufficient to reduce Cyt *c* *in vitro* in the presence of NADPH. The observed Cyt *c* reduction was absolutely dependent on the presence of rAtMFDX1 and rAtMFDR proteins. The Cyt *c* reduction could also be detected with NADH but the rate was considerably low when compared with that obtained with NADPH. This observation was consistent with the higher K_m value of AtMFDR for NADH (123 μM) compared with that for NADPH (11.3 μM).

Subcellular localization

The PSORT program and the TargetP analyses suggested mitochondrial targeting of AtMFDR and AtMFDX proteins, and the N-terminal portions of these proteins seemed to include the properties of mitochondrial transport signal sequences (Glaser *et al.*, 1998). The 100 000 $\times$ *g* pellet from leaf extracts contained a polypeptide immuno-reactive with the anti-rAtMFDR antibodies (Figure 5), indicating membrane association of AtMFDR protein (Figure 7A, lane 6). Mitochondrial localization of AtMFDR was suggested from a subcellular fractionation study (Figure 7B). The anti-rAtMFDR antibodies reacted with a protein of 55 kDa in mitochondrial fractions from *Arabidopsis*, *Brassica pekinensis*, and *B. oleracea* (Figure 7B). The mitochondrial samples used in this study contained significant contamination from chloroplasts as indicated by the immuno-detection of the Rubisco large subunit (Figure 7B, RBCL lanes 3, 4, and 5). However, no immunoreactive protein was seen in the chloroplast fraction when the blot was probed with the anti-rAtMFDR antibodies (Figure 7B, AtMFDR lane 6). These results suggested that AtMFDR protein was primarily localized to the mitochondria.

Figure 7C (right) shows the localization of AtMFDR protein in *Arabidopsis* leaf cells. The Cy3-derived fluorescence observed with the anti-rAtMFDR

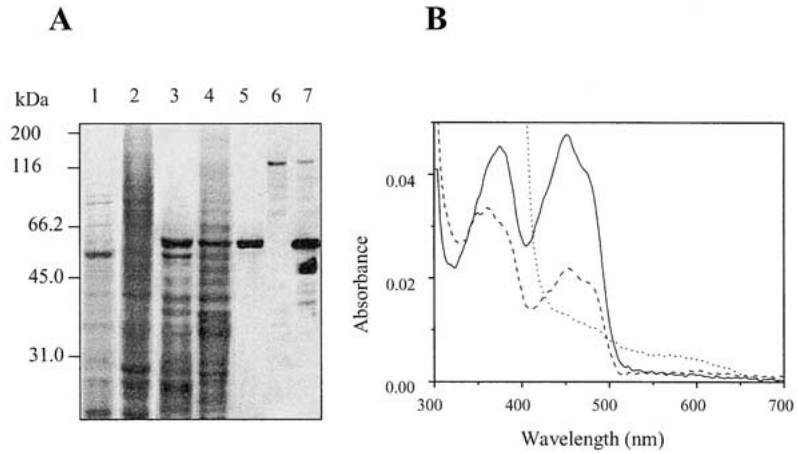

Figure 5. Heterologous expression of the recombinant AtMFDR protein in insect cells. A. SDS-PAGE was done with a 16% w/v polyacrylamide slab gel, and proteins were visualized by staining with Coomassie Brilliant Blue R-250. Lane 1, 100 000 × *g* supernatant from mock-infected Sf9 cells; lane 2, 100 000 × *g* pellet from mock-infected Sf9 cells; lane 3, 100 000 × *g* supernatant from Sf9 cells infected with the recombinant virus containing the full-length AtMFDR cDNA; lane 4, 100 000 × *g* pellet from Sf9 cells infected with the recombinant virus containing the full-length AtMFDR cDNA; lane 5, purified recombinant AtMFDR; lane 6, protein-gel blot analysis of the crude cell extract from the mock-infected Sf9 cells; lane 7, protein-gel blot analysis of the Sf9 cells expressing AtMFDR. Polyclonal antibodies raised against the purified rAtMFDR were used for the immuno-detection at 1:3000 dilution (lanes 6 and 7). The positions of molecular mass markers are shown at the left. B. The absolute absorption spectra of the purified recombinant AtMFDR. Solid line, oxidized form; dashed line, reduced by addition of 100 μM NADH; dotted line, fully reduced state by adding $Na_2S_2O_4$.

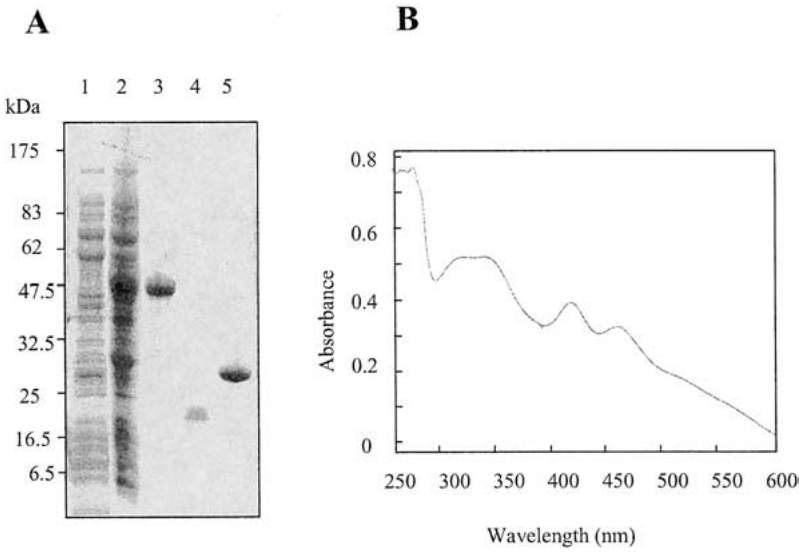

Figure 6. Heterologous expression of *Arabidopsis* AtMFDX1 cDNA in *E. coli*. A. Expression and purification of recombinant AtMFDX1 (rAtMFDX1) protein. SDS-PAGE was done with 5–20% w/v polyacrylamide gradient gel, and proteins were visualized by staining with Coomassie Brilliant Blue R-250. Proteins (10 μg) from untransformed cells were analyzed in lane 1. Crude extract (10 μg protein) from the *E. coli* expressing rAtMFDX1-GST fusion protein was in lane 2. AtMFDX1-GST fusion protein was purified with Glutathione Sepharose 4B (lane 3), and a mature form of rAtMFDX1 protein (lane 4) was obtained after the cleavage using PreScission Protease (Amersham Biosciences) according to the manufacturer's protocol. GST protein after the protease treatment is shown in lane 5. B. Absolute absorption spectra of the mature form of rAtMFDX1.

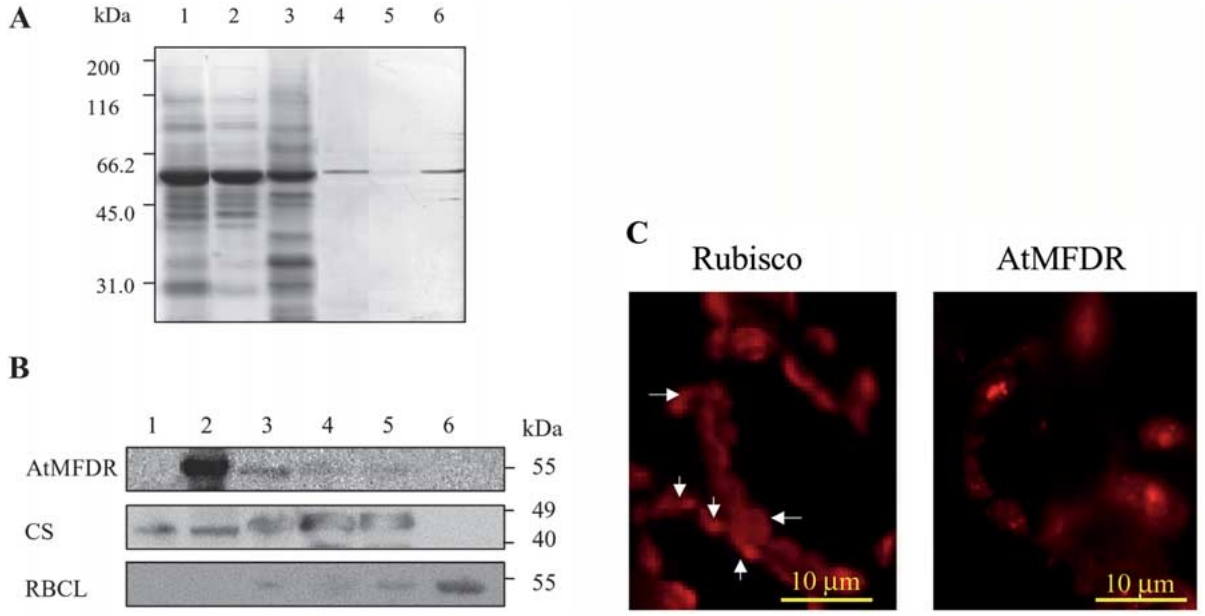

Figure 7. Subcellular localization of AtMFDR. A. Crude leaf extract (lane 1) was centrifuged at 100 000 × *g*. Proteins (10 μg) of the supernatant (lane 2) and the pellet (lane 3) were separated on 16% (w/v) SDS-PAGE and electroblotted onto a nitrocellulose membrane. The blot was analyzed by immunodetection with the anti-rAtMFDR antibodies at 1:3000 dilution. Lane 4 (the crude extract) and lane 6 (the pellet) contained an immuno-reactive band of about 55 kDa, which was not seen in lane 5 (the supernatant). In this experiment, leaf tissues were homogenized with 50 mM Tris-HCl buffer pH 7.8 containing a protease inhibitor cocktail comprised of 4-(2-aminoethyl)benzenesulfonyl fluoride, pepstatin A, bestatin, and Na-EDTA (Sigma Aldrich). The positions of molecular weight markers are shown at the left. B.. Subcellular fractionation. Lane 1, crude extract from sf9 cells; lane 2, crude extract from Sf9 cells expressing rAtMFDR; lane 3, mitochondrial fraction from *Arabidopsis* leaves; lane 4, mitochondrial fraction from *B. pekinensis*; lane 5, mitochondrial fraction from *B. oleracea*; lane 6, chloroplasts from *Arabidopsis* leaves. Proteins (15 μg) were separated by SDS-PAGE and transferred onto a polyvinylidene difluoride membrane for immunodetection with the anti-rAtMFDR antibodies, anti-citrate synthase antibodies (Koyama *et al*., 1999), and anti-spinach Rubisco antibodies (Prof. A. Yokota of Nara Institute of Science and Technology, Japan). The positions of molecular weight markers are shown at the right. C. Tissue immunolabeling experiment. *Arabidopsis* leaf sections were embedded in LR-White resin after the fixation in 50 mM potassium phosphate buffer pH 7.4 containing 16% w/v paraformaldehyde and 2% w/v glutaraldehyde. The anti-AtMFDR and the anti-spinach Rubisco antibodies were used as the primary antibodies, and Cy3-labeled goat anti-rabbit IgG (Jackson Immunoresearch Laboratories) was used for the detection of the primary antibodies. Immunofluorescent images were obtained using a fluorescence microscope (Eclipse E600, Nikon). Some choloroplasts are indicated by white arrows (left, Rubisco). Different subcellular images are observed with the anti-AtMFDR antibodies (right, AtMFDR).

antibodies seemed to be localized to a specific structure, which was clearly different from the localization of Rubisco protein (Figure 7C, left). To provide further evidence that these electron transfer components are localized to mitochondria, we analyzed transient expression of fusion proteins of AtMFDXs/S-GFP and AtMFDR/S-GFP in onion epidermal cells. As shown in Figure 8, fluorescence from the AtMFDX1/S-GFP and the AtMFDR/S-GFP fusions was seen with the organelles which the Mitotracker fluorescence confirmed as mitochondria. Similar images were observed with the expression of AtMFDX2/S-GFP fusion (not shown). These results indicated that the N-terminal peptides (Met-1 to Ile-93 of AtMFDX1) of AtMFDX and AtMFDR (Met-1 to Val-40) were functional and sufficient to transport proteins to mitochondria.

Tissue distribution of AtMFDR *and* AtMFDXs *gene transcripts*

Figure 9A shows that the accumulation levels of *AtMFDR* and *AtMFDX* transcripts were specifically high in flowers, while other tissues contained only lower levels. On the other hand, RT-PCR experiments substantiated the expression of both *AtMFDX* and *AtMFDR* genes in leaf tissues (data not shown). A protein-gel blot analysis revealed significant accumulation of AtMFDR protein in leaf, stem, and flower (Figure 9B). RT-PCR analyses using total RNA from flowers and gene specific primers (Figure 9, C and D) suggested that the expression level of *AtMFDX2* was higher than that of *AtMFDX1*. These results indicated that these electron transfer components were

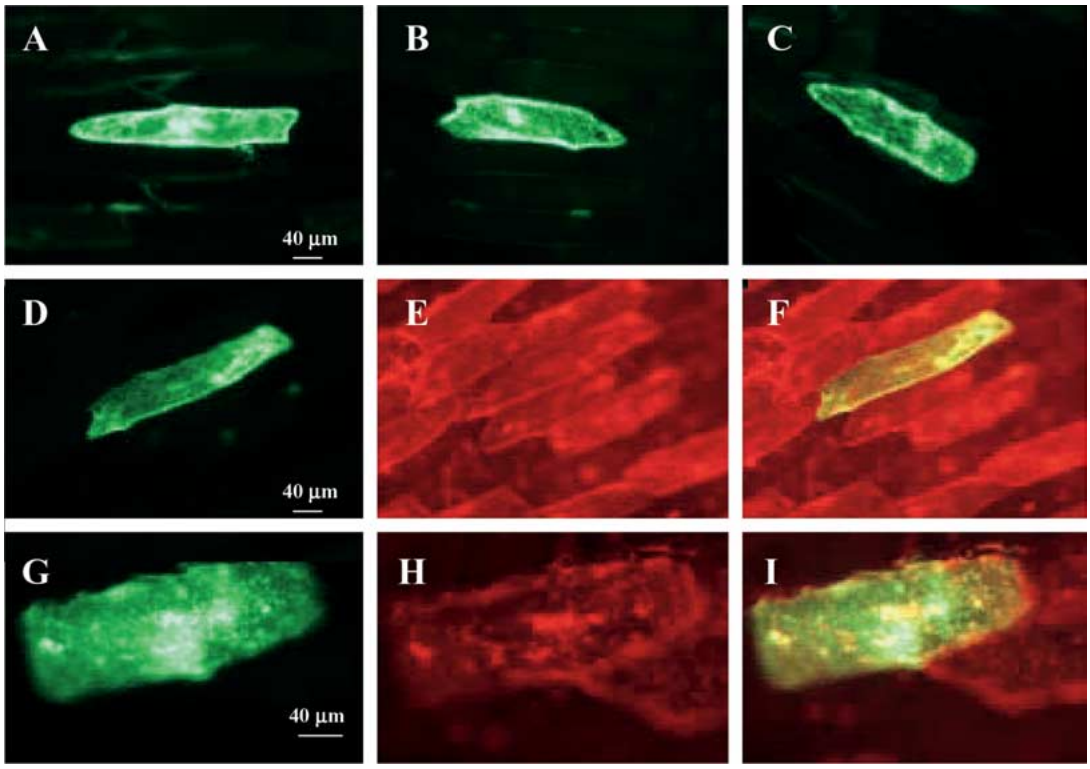

Figure 8. Transient expression of the AtMFDX1/S-GFP and the AtMFDR/S-GFP fusion proteins in onion epidermal cells. Expression of the fusion proteins was under control of the cauliflower mosaic virus 35S promoter and the nopaline synthase terminator. A. Onion epidermal cells transformed with sGFP(S65T). B. AtMFDX1/S-GFP. C. AtMFDR/S-GFP fusion proteins. AtMFDX1/S-GFP-expressing cells (D) were treated with the mitochondria-specific dye MitoTracker Red cmXRos (E). F. Image obtained by merging the GFP fluorescence (D) and the MitoTracker Red fluorescence (E). AtMFDR/S-GFP-expressing cells (G) were also treated with Mitotracker, and the Red fluorescence image (H) was merged (I) with GFP fluorescence (G). Fluorescence of GFP and Mitotracker Red visualized with an Olympus microscope IX71 (Olympus, Tokyo, Japan) and the following filter sets of U-MGFPHQ for GFP and U-MWIG2 for MitoTracker. Images were taken with the DP manager software (Olympus).

functioning not only in flowers but also in every tissue throughout development.

Discussion

Ferredoxins and ferredoxin reductases are widely distributed in organisms across kingdoms and are involved in a variety of metabolic processes (Arakaki *et al*., 1997). In photosynthetic organisms, these electron transfer components participate in the generation of NADPH during the linear photosynthetic electron transport. On the other hand, plant plastidal ferredoxin and ferredoxin reductase in non-photosynthetic tissues play crucial roles in nitrogen assimilation. In mammals, ADX and ADR constitute the mitochondrial electron transfer system for the P450-dependent steroid hydroxylation (Vickery, 1997). However, no mitochondrial ferredoxins and ferredoxin reductases from plants have so far been elucidated.

In *Arabidopsis*, we identified and characterized the genes encoding mitochondrial types of ferredoxins (AtMFDX1 and AtMFDX2) and ferredoxin reductase (AtMFDR). cDNA cloning and recombinant protein studies demonstrated that these genes encode functionally active proteins. Subcellular localization studies and the transient expression of GFP fusions indicated that these electron transfer components are localized to mitochondria, suggesting that AtMFDXs and AtMFDR could be physiologically related redox proteins in plant mitochondria. Considering the mammalian ADX and ADR functions, it is possible that AtMFDX and AtMFDR may be involved in the P450 monooxygenase reactions in plants. In fact, AtMFDX and AtMFDR proteins conserved the amino acid residues (Figures 1 and 3) implicated in the interaction with mitochondrial P450s (Grinberg *et al*.,

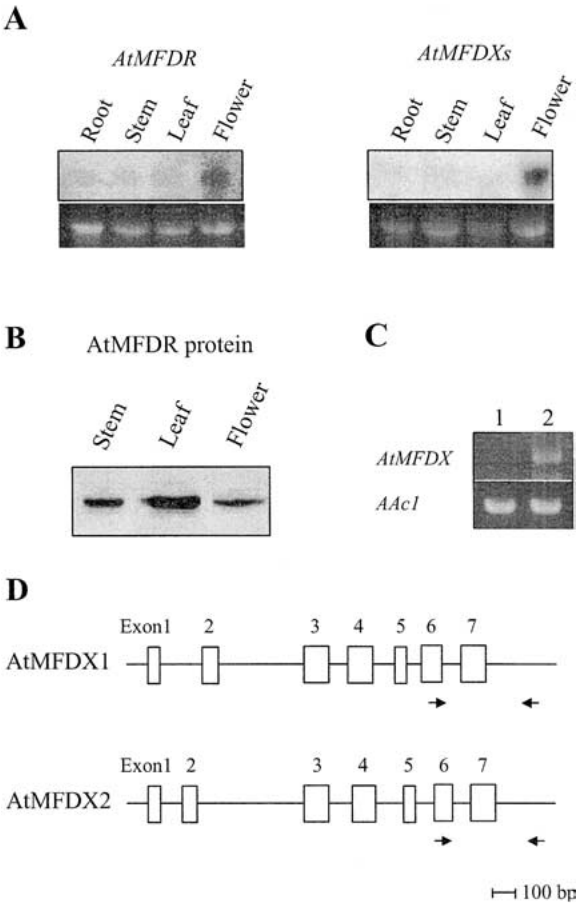

Figure 9. Tissue distribution of the gene transcripts. A. Total RNA was isolated from roots and leaves of 3-week old plants, and from inflorescence stems and flowers of 5-week old plants. Total RNA (10 μg) was probed with either the full-length cDNA of AtMFDX1 or AtMFDR. B. Accumulation levels of AtMFDR protein in stem, leaf, and flower. Tissues were homogenized with 50 mM Tris-HCl buffer pH 7.8 containing a protease inhibitor cocktail (Sigma Aldrich). Proteins (10 μg) were separated on 16% w/v SDS-PAGE and electroblotted onto a PVDF membrane. The blot was analyzed by immunodetection using the anti-rAtMFDR antibodies and the ECL detection system (Amersham Biosciences). C. RT-PCR analysis was done to examine the accumulation levels of *AtMFDX1* and *AtMFDX2* gene transcripts. The *Arabidopsis* actin gene (*AAc1*; Nairn *et al.*, 1988) was amplified by RT-PCR as the internal control. D. Schematic diagrams to illustrate RT-PCR amplification. The forward primer and the reverse primers were derived from exon 6 and the 3′-untranslated region, respectively, thereby ensuring the identification of the PCR fragment amplified from the first-strand cDNA as the template. The exons are indicated by the open boxes.

2000). However, we were not successful in reconstituting *in vitro* the monooxygenase reaction of a bovine adrenal P450 (CYP11B2, Nonaka *et al.*, 1998) using rAtMFDX1 and rAtMFDR proteins. No P450 protein has so far been identified in the mitochondrial proteome (Kruft *et al.*, 2001; Millar *et al.*, 2001), and mitochondrial P450 systems in plants still remain to be clarified.

Millar *et al.* (2001), have identified an adrenodoxin/mitochondrial ferredoxin homologue (TrEMBL accession number Q9SRR8 encoded by AT3g07480) in the *Arabidopsis* mitochondrial proteome. In the phylogenetic tree (Figure 2), this ADX homologue (Q9SRR8 protein) was not in the mitochondrial ferredoxin group but very close to putidaredoxin involved in the P450cam reaction of *Pseudomonas putida* (Shimada *et al.*, 2001). A sequence comparison revealed that Q9SRR8 protein is missing one of the four Cys residues involved in the [2Fe-2S] cluster binding (Arakaki *et al.*, 1997; Grinberg *et al.*, 2000). Since the ORF for Q9SRR8 protein consists of a single exon, the annotation of AT3g07480 should not have had an error by overlooking additional exons for the missing Cys residue. In addition, this protein sequence does not include the acidic amino acid residues involved in the interaction with ferredoxin reductase (Grinberg *et al.*, 2000). These observations indicated that this ADX homologue could not function in the mitochondrial P450 monooxygenase reactions but instead plays a part in different metabolic processes.

In prokaryotic microorganisms (Lill and Kispal, 2000), the assembly of the Fe-S cluster is mediated by the functions of a series of proteins including a [2Fe-2S] ferredoxin encoded by the *isc* operon. A process similar to that mediated by the prokaryotic *isc*-encoded proteins including NifU is also operating in mitochondria of eukaryotic cells (Lange *et al.*, 2000; Mühlenhoff and Lill, 2000). Thus, Yah1p (Lange *et al.*, 2000) and Arh1p (Li *et al.*, 2001) are the homologues of ADX and ADR in yeast, respectively, and participate in the Fe-S cluster maturation and mitochondrial iron homeostasis. It has been reported that mitochondria of human cells contains an analogous system for Fe-S cluster maturation (Tong and Rouault, 2000). It has recently been reported that the *STARIK* gene in *Arabidopsis* encodes a half-type ABC transporter, a functional homologue of yeast Atm1p involved in the export of mature Fe-S clusters from mitochondria (Kushnir *et al.*, 2001). The *Arabidopsis* genome contains putative genes for proteins homologous to those involved in the microbial

Fe-S cluster maturation processes (Lill and Kispal, 2000). For example, AT5g65720 is thought to encode a cysteine desulphrase (NifS-like) involved in the initial step of the Fe-S cluster biosynthesis. Kushnir *et al*. (2001) reported that this NifS-like protein was targeted to mitochondria. In addition, *Arabidopsis* genes (AT4g22220, AT4g04080, and AT3g01020) are predicted to encode NifU-like protein, a component for the Fe-S maturation process. It is therefore possible that AtMFDXs and AtMFDR may be involved in the process of Fe-S maturation process as found in other organisms. On the other hand, it has been reported that another NifS-like cysteine desulfhydrase (AtNFS2, At1g08490) in *Arabidopsis* was targeted to plastids (Léon *et al*., 2002), indicating that the Fe-S biosynthesis in plants is not as simple as that found in yeast.

The current results indicate that AtMFDX and AtMFDR are localized to mitochondria, and physiological redox partners functioning with AtMFDX and AtMFDR should also be present at the same subcellular localization. Extensive mitochondrial proteomics studies or protein interaction studies together with the elucidation of submitochondrial localization of these electron transfer components will provide essential information to understand the physiological functions of AtMFDXs and AtMFDR with terminal electron acceptor proteins.

Acknowledgements

We thank Hiroyuki Koyama of Gifu University for the gift of the anti-citrate synthase antibodies. We thank Akiho Yokota of Nara Institute of Science and Technology for anti-spinach Rubisco antibodies. We are grateful to Yasuo Niwa of Shizuoka Prefecture University for the gift of the sGFP(S65T) gene. We thank Takashi Aoyama of Kyoto University for valuable discussion and the use of the Biolistic microprojectile device. This work was supported in part by the Ministry of Education, Culture, Sports, Science, and Technology of Japan (grant 14560288 to D.O.). A part of this work was performed as a part of the R&D Project of Industrial Science and Technology Frontier Program supported by NEDO (New Energy and Industrial Technology Development Organization).

References

Arakaki, A.K., Ceccarelli, E.A. and Carrillo, N. 1997. Plant-type ferredoxin-NADP$^+$ reductases: a basal structural framework and a multiplicity of functions. FASEB J. 11: 133–140.

Barros, M.H. and Nobrega, F.G. 1999. YAH1 of *Saccharomyces cerevisiae*: a new essential gene that codes for a protein homologous to human adrenodoxin. Gene 233: 197–203.

Barros, M.H., Nobrega, F.G. and Tzagoloff, A. 2002. Mitochondrial ferredoxin is required for heme A synthesis in *Saccharomyces cerevisiae.* J. Biol. Chem. 277: 9997–10002.

Chiu, W., Niwa, Zeng, YW., Hirano, T., Kobayashi, H. and Sheen, J. 1996. Engineered GFP as a vital reporter in plants. Curr. Biol. 6: 325–330.

Chu, J.W. and Kimura, T. 1973. Studies on adrenal steroid hydroxylases. Molecular and catalytic properties of adrenodoxin reductase (a flavoprotein). J. Biol. Chem. 248: 2089–2094.

Felsenstein, J. 1996. Inferring phylogenies from protein sequences by parsimony, distance, and likelihood methods. Meth. Enzymol. 266: 418–427.

Fujimori, K. and Ohta, D. 1998. Isolation and characterization of a histidine biosynthetic gene in *Arabidopsis* encoding a polypeptide with two separate domains for phosphoribosyl-ATP pyrophosphohydrolase and phosphoribosyl-AMP cyclohydrolase. Plant Physiol. 118: 275–283.

Fukuchi-Mizutani, M., Mizutani, M., Tanaka, Y., Kusumi, T. and Ohta, D. 1999. Microsomal electron transfer in higher plants: cloning and heterologous expression of NADH-cytochrome *b*5 reductase from *Arabidopsis*. Plant Physiol. 119: 353–362.

Glaser, E., Sjoling, S., Tanudji, M. and Whelan, J. 1998. Mitochondrial protein import in plants. Signals, sorting, targeting, processing and regulation. Plant Mol. Biol. 38: 311–338.

Grinberg, A.V., Hannemann, F., Schiffler, B., Müller, J., Heinemann, U. and Bernhardt, R. 2000. Adrenodoxin: structure, stability, and electron transfer properties. Proteins 40: 590–612.

Huang, J.J. and Kimura, T. 1973. Studies on adrenal hydroxylases. Oxidation-reduction properties of adrenal iron-sulfur protein (adrenodoxin). Biochemistry 12: 406–409.

Kagimoto, M., Kagimoto, K., Simpson, E.R., and Waterman, M.R. 1988. Transcription of the bovine adrenodoxin gene produces two species of mRNA of which only one is translated into adrenodoxin. J. Biol. Chem. 263: 8925–8928.

Klein, M., Binder, S. and Brennicke, A. 1998. Preparation of mitochondria from *Arabidopsis*. In: J.M. Martínez-Zapater and J. Salinas (Eds.) Arabidopsis Protocols, Humana Press, Totowa, NJ, pp. 49–53.

Koyama, H,, Takita, E., Kawamura, A., Hara, T. and Shibata, D. 1999. Over expression of mitochondiral citrate synthase gene improves the growth of carrot cells in Al-phosphate medium. Plant Cell Physiol. 40: 482–488.

Krömer, S. and Heldt, H.W. 1991. Respiration of pea leaf mitochondria and redox transfer between the mitochondrial and extramitochondrial compartment. Biochim. Biophys. Acta 1057: 42–50.

Kruft, V., Eubel, H., Jänsch, L., Werhahn, W. and Braun, H.-P. 2001. Proteomic approach to identify novel mitochondrial proteins in *Arabidopsis*. Plant Physiol. 127: 1694–1710.

Kunst, L. 1998. Preparation of physiologically active chloroplasts from *Arabidopsis*. In: J.M. Martínez-Zapater and J. Salinas (Eds.) Arabidopsis Protocols, Humana Press, Totowa, NJ, pp. 43–48.

Kushnir, S., Babiychuk, E., Storozhenko, S., Davey, M., Papenbrock, J., De Rycke, R. R., Engler, G., Stephan, U., Lange, H., Kispal, G., Lill, R. and Van Montagu, M. 2001. A mutation of

the mitochondrial ABC transporter *Sta1* leads to dwarfism and chlorosis in the *Arabidopsis* mutant *starik*. Plant Cell 13: 89–100.

Lacour, T., Achstetter, T. and Dumas, B. 1998 Characterization of recombinant adrenodoxin reductase homologue (Arh1p) from yeast. Implication in *in vitro* cytochrome p45011β monooxygenase system. J. Biol. Chem. 273: 23984–23992.

Laemmli, U.K. 1970. Cleavage of structural proteins during the assembly of the head of bacteriophage T4. Nature 227: 680–685.

Lange, H., Kaut, A., Kispal, G. and Lill, R. 2000. A mitochondrial ferredoxin is essential for biogenesis of cellular iron-sulfur proteins. Proc. Natl. Acad. Sci. USA. 97: 1050–1055.

Léon, S., Touraine, B., Briat, J.-F. and Lobréaux, S. 2002. The *AtNFS2* gene from *Arabidopsis thaliana* encodes a NifS-like plastidal cysteine desulphurase. Biochem. J. 366: 557–564.

Li, J., Saxena, S., Pain, D. and Dancis, A. 2001. Adrenodoxin reductase homolog (Arh1p) of yeast mitochondria required for iron homeostasis. J. Biol. Chem. 276: 1503–1509.

Lill, R. and Kispal, G. 2000. Maturation of cellular Fe-S proteins: an essential function of mitochondria. Trends Biochem. Sci. 25: 352–356.

Manzella, L., Barros, M.H. and Nobrega, F.G. 1998. ARH1 of *Saccharomyces cerevisiae*: a new essential gene that codes for a protein homologous to the human adrenodoxin reductase. Yeast 14: 839–846.

Millar, A.H., Sweetlove, L.J., Giegé, P. and Leaver, C.J. 2001. Analysis of the *Arabidopsis* mitochondrial proteome. Plant Physiol. 127: 1711–1727.

Mizutani, M., Ohta, D. and Sato, R. 1997. Isolation of a cDNA and a genomic clone encoding cinnamate 4-hydroxylase from *Arabidopsis* and its expression manner in planta. Plant Physiol. 113: 755–763.

Mizutani, M. and Ohta, D. 1998. Two isoforms of NADPH:cytochrome P450 reductase in *Arabidopsis thaliana*. Gene structure, heterologous expression in insect cells, and differential 28 regulation. Plant Physiol. 116: 357–367.

Mühlenhoff, U. and Lill, R. 2000. Biogenesis of iron-sulfur proteins in eukaryotes: a novel task of mitochondria that is inherited from bacteria. Biochim. Biophys. Acta 1459: 370–382.

Müller, J.J., Lapko, A., Bourenkov, G., Ruckpaul, K. and Heinemann, U. 2001. Adrenodoxin reductase-adrenodoxin complex structure suggests electron transfer path in steroid biosynthesis. J. Biol. Chem. 276: 2786–2789.

Nairn, C.J., Winesett, L. and Ferl, R.J. 1988. Nucleotide sequence of an actin gene from *Arabidopsis thaliana*. Gene 65: 247–257.

Neuberger, M., Journet, E.-P., Bligny, R., Carde, J.P. and Douce, R. 1982 Purification of plant mitochondria by isopycnic centrifugation in density gradients of Percoll. Arch. Biochem. Biophys. 217: 312–323.

Nonaka, Y., Murakami, H., Yabusaki, Y., Kuramitsu, S., Kagamiyama, H., Yamano, T. and Okamoto, M. 1987. Molecular cloning and sequence analysis of full-length cDNA for mRNA of adrenodoxin oxidoreductase from bovine adrenal cortex. Biochem. Biophys. Res. Commun. 145: 1239–1247.

Nonaka, Y., Fujii, T., Kagawa, Y., Waterman, M.R., Takemori, H. and Okamoto, M. 1998. Structure/function releationship of CYP11B1 assocated with Dahl's salt-resistant rats Expression of rat CYP11B1 and CYP11B2 in *Escherichia coli*. Eur. J. Biochem. 258: 869–878.

Shimada, H., Nagano, S., Hori, H. and Ishimura, Y. 2001. Putidaredoxin-cytochrome P450cam interaction. J. Inorg. Biochem. 83: 255–260.

Takahashi, Y. and Nakamura, M. 1999. Functional assignment of the ORF2-*iscS-iscU-iscA-hscB-hscA-fdx*-ORF3 gene cluster involved in the assembly of Fe-S clusters in*Escherichia coli*. J. Biochem. 126: 917–926.

Thompson, J.D., Higgins, D.G. and Gibson, T.J. 1994. CLUSTAL W: improving the sensitivity of progressive multiple sequence alignment through sequence weighting, position-specific gap penalties and weight matrix choice. Nucl. Acids. Res. 22: 4673–4680.

Tong, W.H. and Rouault, T. 2000. Distinct iron-sulfur cluster assembly complexes exist in the cytosol and mitochondria of human cells. EMBO J. 21: 5692–5700.

Urban, P., Mignotte, C., Kazmaier, M., Delorme, F. and Pompon, D. 1997. Cloning, yeast expression, and characterization of the coupling of two distantly related *Arabidopsis thaliana* NADPH-cytochrome P450 reductases with P450 CYP73A5. J. Biol. Chem. 272: 19176–19186.

Vickery, L.E. 1997. Molecular recognition and electron transfer in the mitochondrial steroid hydroxylase system. Steroids 62: 124–127.

Walker, D.A. 1980. Preparation of higher plant chloroplasts. Meth. Enzymol. 69: 94–104.

Xia, B., Cheng, H., Bandarian, V., Reed, G.H. and Markley, J.L. 1996. Human ferredoxin: overproduction in *Escherichia coli*, reconstitution *in vitro*, and spectroscopic studies of iron-sulfur cluster ligand cysteine-to-serine mutants. Biochemistry 35: 9488–9495.

Ziegler, G.A., Vonrhein, C., Hanukoglu, I. and Schulz, G.E. 1999. The structure of adrenodoxin reductase of mitochondrial P450 systems: electron transfer for steroid biosynthesis. J. Mol. Biol. 289: 981–990.

Ziegler, G.B. and Schulz, G.E. 2000. Crystal structures of adrenodoxin reductase in complex with $NADP^+$ and NADPH suggesting a mechanism for the electron transfer of an enzyme family. Biochemistry 39: 10986–10995.